Characterization of Mo-Re/ZSM-5 Catalysts: How the Rhenium Improves the Performance of Mo in the Methane Dehydroaromatization Reaction

A. López-Martín[a], M.F. Sini[b], M.G. Cutrufello[b], A. Caballero[a†] and G. Colón[a†]

[a] *Instituto de Ciencia de Materiales de Sevilla. Centro Mixto Universidad de Sevilla-CSIC.*

Américo Vespucio s/n. 41092 Sevilla. Spain

[b] *Dipartimento di Scienze Chimiche e Geologiche. Università di Cagliari.*

Complesso Universitario Monserrato, SS 554 Bivio Sestu. 09124 Cagliari, Italy

[†] corresponding authors: caballero@us.es and gcolon@icmse.csic.es

Abstract

In this study, the promoting effect of rhenium addition as a co-dopant on Mo/ZSM-5 catalysts system has been analysed. Hence, bimetallic (Re-Mo/ZSM-5) catalysts have been synthesized using a sequential impregnation methodology. The catalytic performance for direct aromatization of methane reaction has been determined and correlated with their physical and chemical state combining multiple characterization techniques. An important synergy between Mo and Re, affected by the sequential impregnation, has been observed. Thus, Re1-Mo4/ZSM-5 in which rhenium has been incorporated first shows notably higher aromatic yields and stability against deactivation. Characterization results suggest that catalytic enhancement is due to the important effect of Re presence in close interaction with Mo. Improved evolution of ethane through C-C coupling would be correlated to this catalytic performance. As we discuss, Mo nature and location in the bimetallic systems are strongly conditioned by Re and the impregnation sequence and favours such intermediate step.

Keywords: bimetallic, molybdenum, rhenium, methane dehydroaromatization.

Introduction

Non-oxidative catalytic methane dehydroaromatization (*MDA*) to benzene provides a potential route for direct production of benzene from methane resources. *MDA* was first reported more than 25 years ago by Wang *et al* [1], and the increasing availability of cheap natural gas has attracted growing interest at this direct route for the conversion of methane into high-value chemicals [2]. Several research works have been published on this topic in the last few decades. However Mo/HZSM-5, found by Wang in 1993, is still the preferred catalyst for *MDA* reaction [3]. Challenges with the MDA reaction are two-fold: the reaction is thermodynamically limited with low one-pass methane conversion and even the best catalytic systems, Mo/zeolites, suffer rapid deactivation from coking [4]. Within this framework, several characteristics are yet unknown and how to prevent its deactivation caused by coke formation still remains an unsolved problem that hinders its industrial application [5,6,7].

In order to improve the catalytic performance and to decrease the deactivation rate, multiple studies have reported the addition of different metals as a co-dopants to the Mo catalysts. However, though reported results showed interesting effects, attained improvements appears always temporary and the stability of the catalysts was always a challenge [8]. For this sake, a catalyst design strategy is crucial to improve stability. So, the use of multifunctional Mo-X/zeolite systems, where X is a co-dopant capable of modulating the stability, has been widely reported. In this sense, the addition of metal dopants to would improve not only the catalytic performance but also the stability of Mo/ZSM-5 catalysts by influencing the catalyst deactivation step.

Thus, Scurrell and co-workers added platinum and/or tin on Mo/ZSM-5 zeolite catalyst for methane aromatization reaction [9]. They concluded that catalysts with additional tin led to lower methane conversion but higher aromatic products selectivity. Abdelsayed *et al* introduced Fe

and/or Zn to modify conventional Mo/ZSM-5 catalysts, demonstrating that Fe-Mo/ZSM-5 displayed high stability and selectivity to aromatics [10]. Zhang *et al* studied the effect of indium on Mo/ZSM-5 in *MDA* concluding that although methane conversion decreases, the coke selectivity is reduced to 50% that of Mo/ZSM-5 [11]. Such stabilization seems to be related to the close proximity of In and Mo that would suppress coke formation. More recently, Sridhar *et al* reported the addition of different loadings of Co and Ni on Mo/ZSM-5 catalyst in order to evaluate the promoting effect of these metals on reactivity and stability of the Mo catalysts [12]. They observed a synergistic effect between Mo and the promoters, resulting in benzene yield and catalytic stability improvements.

Since it is proposed that Brønsted acid sites would play an important role in the reaction pathways, the modification of the zeolite acidity would be achieved through metal co-doping [13]. Thus, Cr, Ag and Ga were employed as additive that increased the catalyst acidity and resulted in improved methane conversion and benzene selectivity [8].

In this paper we study the effect of rhenium addition as co-dopant to the classical Mo/ZSM-5 catalyst, and how it affects, on the one hand to the physicochemical properties, and on the other hand to the catalytic activity and stability during *MDA* reaction. We show the important effect of the sequential addition of metals, preparing two different series of catalyst in which Mo has been loaded first in a case (Mo1st), and Re in the other (Re1st). Both catalyst series have been widely characterized by several techniques, in particular XPS and TPR, and also tested in order to evaluate its catalytic performance in the *MDA* reaction.

Experimental Section

Catalyst preparation.

The mono- and bimetallic catalysts were prepared using a commercial NH_4-ZSM-5 zeolite (Alfa Aesar, Si/Al=23/1) previously calcined at 550 ºC for 3 hours to obtain the acid form. In the case of bimetallic systems, Mo and Re were sequentially added by impregnation procedure. Thus for each series, one of the metal was firstly impregnated and the sample was calcined at 550 ºC, 3h. After which, the second metal was subsequently introduced and the solid further calcined again at the same temperature. The obtained series of catalysts were named as Mo1st and Re1st.

Molybdenum was loaded using ammonium heptamolybdate tetrahydrate of appropriate concentration ($(NH_4)_6Mo_7O_{24}\cdot 4H_2O$, Sigma Aldrich) to obtain 4 wt% Mo, while rhenium was loaded using rhenium (VII) oxide (Re_2O_7, Sigma Aldrich) at the corresponding stoichiometric amount leading to 1 wt% and 4 wt%. As a result, the following bimetallic systems were obtained: Re1-Mo4 and Re4-Mo4.

Catalytic activity in the Methane Dehydroaromatization (MDA).

The experimental measurements were accomplished with 0.1 g of catalyst diluted in 0.1 g of SiC, using a stainless-steel tubular reactor equipped with a temperature controller and four mass flow controllers. The stainless-steel reactor without catalyst, charged just with 0.2 g of SiC, was completely inactive for the *MDA* reaction. Before reaction, catalysts were pretreated under O_2/N_2 (20% in O_2) flow of 15 mL/min at 250 ºC for 1 h. Then the temperature was lowered to 150 ºC under inert gas. For methane dehydroaromatization reaction CH_4 /N_2 (85%) flow was introduced in the reactor at 5mL/min, and temperature was then ramped up with a rate of 10 ºC/ min from 150 ºC until 700 ºC, and held at this temperature for 18 h. Reactants and reaction products were

monitored by means of a previously calibrated GC 7890B using TCD (Molsieve and HayeSep Q columns, for H_2 and permanent gases) and FID (GS-GasPro and HP88 columns, for HCs and aromatics) detectors. All lines connecting the reactor and GC were heated in order to avoid condensation of products.

Conversion and selectivity values were calculated according to the following mathematical expressions:

$$Conversion(\%) = \frac{[CH_4]_t}{[CH_4]_i} \times 100 \text{ ,}$$

where $[CH_4]_t$ represent the moles of reacted methane and $[CH_4]_i$ the initial methane amount.

$$Selectivity\ to\ product\ i(\%) = \frac{[product_i]_t \times n_i}{\sum [product_i]_t \times n_i} \times 100 \text{ ,}$$

where $[product_i]_t$ represents the moles of the specific product, n_i the number of C atoms in the product molecule (6 for benzene) and $\sum[product]_i$ the sum of moles from all products in the reaction. The aromatic selectivity has been determined as the sum of benzene, naphthalene and toluene.

Finally, we have also calculated the accumulated yield for each product obtained (Y_{product_i}) by using the following equation:

$$Y_{product_i}(\mathrm{mmol}/g_{cat}) = \sum([\mathrm{product}_i]_t \times C)$$

where $[product_i]_t$ is the products mol at a time *t,* and *C* is a constant which accounts different operational factors as the catalyst mass, the loop volume and time between each GC analysis.

Characterization techniques.

BET surface area measurements were carried out by N_2 adsorption at -196 ºC using a Micromeritics Tristar II instrument. Micropore areas were calculated from the t-plot.

Thermal programmed reduction (TPR) analysis were carried out using a Quantachrome Chemstar instrument equipped with a thermal conductivity detector and a mass spectrometer. About 40 mg of catalyst was first heated to 150 °C in an inert flow of Ar at 30 mL/min for 60 min previous to each experiment. The experimental conditions were chosen to fulfil the resolution conditions, according to the indication included in a previous work [14,15].

Ammonia adsorption microcalorimetry measurements were performed with a Tian-Calvet heat flow microcalorimeter (Setaram), equipped with a volumetric vacuum line. Each sample (ca. 0.1 g, 40-80 mesh) was thermally pretreated at 80 °C for 12 h under vacuum (5 mPa). Ammonia adsorption was carried out by admitting successive doses of the probe gas and measuring the equilibrium pressure relative to each adsorbed amount by means of a differential pressure gauge (Datameritics) up to a final equilibrium pressure of about 133 Pa. The thermal effect corresponding to the adsorption of each dose was simultaneously recorded. The adsorption temperature was kept at 80 °C, in order to limit physisorption. After overnight outgassing at the same temperature, a readsorption run was carried out, in order to distinguish the acid sites weak enough to be made free through the outgassing step. The adsorption and calorimetric isotherms were obtained from each adsorption (and readsorption) experiment. Combining the two sets of data, a plot of the differential heat of adsorption, Q_{diff}, as a function of the adsorbed amount was drawn, which gives information on the strength distribution of the adsorbing sites.

X-ray photoelectron spectroscopy (XPS) data were recorded on pellets which were outgassed in the prechamber of the instrument at room temperature up to a pressure below $2 \cdot 10^{-8}$ torr to remove chemisorbed water. Thermal treatments were accomplished in a cell directly attached to the main chamber, allowing treatment while in contact with a mixture of gases emulating the TPR experiments. Transfer to the main chamber were accomplished under vacuum conditions, where

spectra were recorded using a VG Scalab 210 spectrometer, working with constant pass energy of 50 eV. The spectrometer main chamber, working at a pressure below $2 \cdot 10^{-9}$ torr, is equipped with a Specs Phoibos 100 hemispherical electron analyser with a dual X-ray source working with Mg Kα (hν= 1254 eV) at 120 W and 30 mA. Si *2p* signal (103.0 eV) was used as the internal energy reference in all the experiments.

The transmission electron microscopy (TEM) images, high angle annular dark field (HAADF) and element mapping analysis images were obtained on the equipment FEI S/TEM Talos F200S. Samples were prepared by dipping a carbon grid in to the powder sample.

Results and Discussion

Methane dehydroaromatization (MDA)

The first important issue to point out is that Re incorporation significantly improves the benzene/aromatic yield in both series with respect to Mo monometallic system. We have to consider that monometallic Re4 catalyst show a very scarce conversion (**Figure 1**), so important synergistic effect can be envisaged in the bimetallic systems.

Moreover, it is worthy to note that the catalytic activity for methane aromatization to benzene reveals that the addition sequence followed would have a marked effect. Thus, Re1st series shows better catalytic performance with respect to Mo1st one. The maximum activity is attained by Re1-Mo4/ZSM-5 catalyst in the Re1st series, for which higher production of benzene and aromatics has been found (**Figure 1**). It is also worth of noting that the increasing amount of Re does not affect to the yield of benzene in the Re1st series. On the contrary, for Mo1st series increasing amount of Re seem to be detrimental. Moreover, in the case of aromatics production, irrespective of the sequence addition, higher Re content leads to a slightly lower yield.

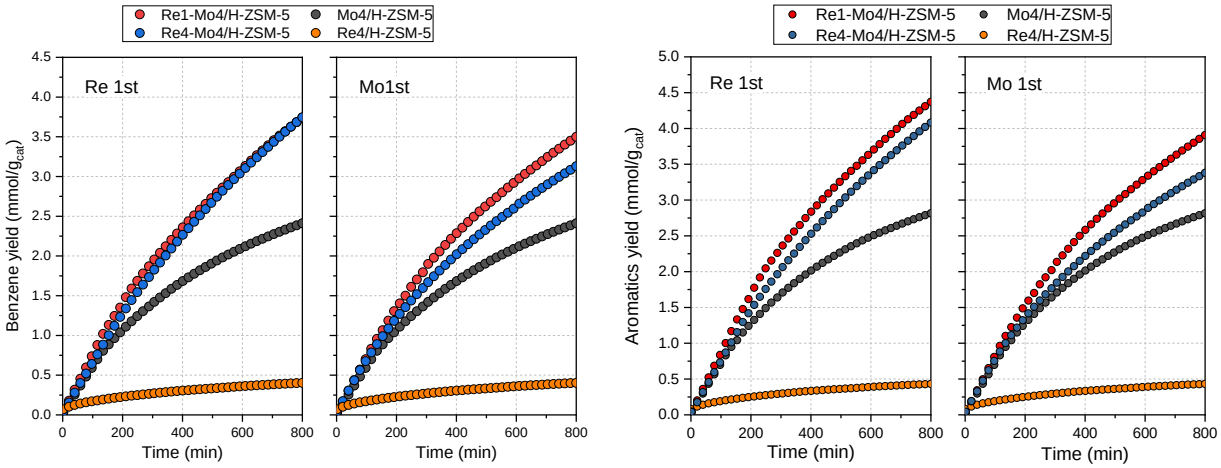

Figure 1. Accumulated benzene and aromatics yields for Mo4/ZSM-5, Re4/ZSM-5 and bimetallic catalysts for Mo1st and Re1st series.

Thus, from both results it can be argued that since benzene yield is similar for bimetallic systems in the Re1st series, the naphthalene production would be slightly favoured in the Re1-Mo4/ZSM-5 with respect the other systems (**Figure S1**). Toluene is residually detected for Re1-Mo4/ZSM-5 systems.

Specifically, after 800 min in stream the obtained aromatics yield was 4.4 mmol/g_{cat} for the Re1-Mo4/ZSM-5 within Re1st series, being significantly higher than the observed value using Mo4/ZSM-5 sample, for which 2.5 mmol/g_{cat} is obtained. The Re incorporation as promoter implies an enhancement of ca 50% with respect to the monometallic system. This is an outstanding improvement if we compare with reported results by other promoters such as Fe [16], Co [17] or Ni [18].

Another interesting aspect concerns the evolution of intermediates. Early proposed mechanism argued that methane would react on the Mo sites to produce ethylene, which further proceeds on the acid sites of the two catalysts to form aromatics (both benzene and coke precursors). In a first

step, ethane could be formed from methane coupling reaction [19]. Then, in a second step, ethane would undergo dehydrogenation to ethylene.

However, a recent report questioned the bifunctional mechanism in which ethylene would be the primary intermediate [15]. Vollmer *et al* proposed that ethylene would not be the major reaction intermediate since the hydrocarbon pool formed in the zeolite matrix during MDA is comprised of less dense and more hydrogenated species than the pool formed from ethylene. The hydrocarbon pool would be formed during the kinetic induction period and consist on compounds trapped within the voids. This hydrocarbon pool mechanism contradicts the well stablished bifunctional mechanism. In this sense, Gu *et al* argued that Bronsted acids predominantly serve as the anchoring points for the dispersion of Mo-species, but their participation in aromatization step is quite limited [20]. On this basis, aromatization is supposed to be the intrinsic property of (oxy-) carbidic Mo sites.

If we observe the production of these intermediates for both series (**Figure 2**), it is clear that while ethylene formation is not notably affected by the presence of Re nor the preparation sequence, in the case of ethane important differences can be observed. Furthermore, the enhanced formation of ethane in Re1-Mo4/ZSM-5 catalyst is accompanied by the higher production of aromatics. Such different evolution would point out the fact that ethylene is not the primary but a side intermediate formed. Moreover, ethylene follows a growing evolution with time, pointing out that is not affected by catalyst deactivation. It is supposed that catalyst deactivation would take place over metal sites by coke deposition. Thus, the formation of ethylene would not be associated to these sites.

Indeed, in a recent kinetic study Razdan *et al*, proposed that ethane is the initial product of C–C coupling [21]. The occurrence of Re and particularly when incorporated first, would be directly associated to the enhanced ethane evolution. Thus, it can be assumed that the differences in the

aromatics production could be consequently associated in part to the best performance in C-C coupling step to ethane. Then, ethylene formation as a secondary intermediate, that is formed equally in all catalysts and therefore is not conditioned by Re presence, seems not to be related with the final aromatics formation.

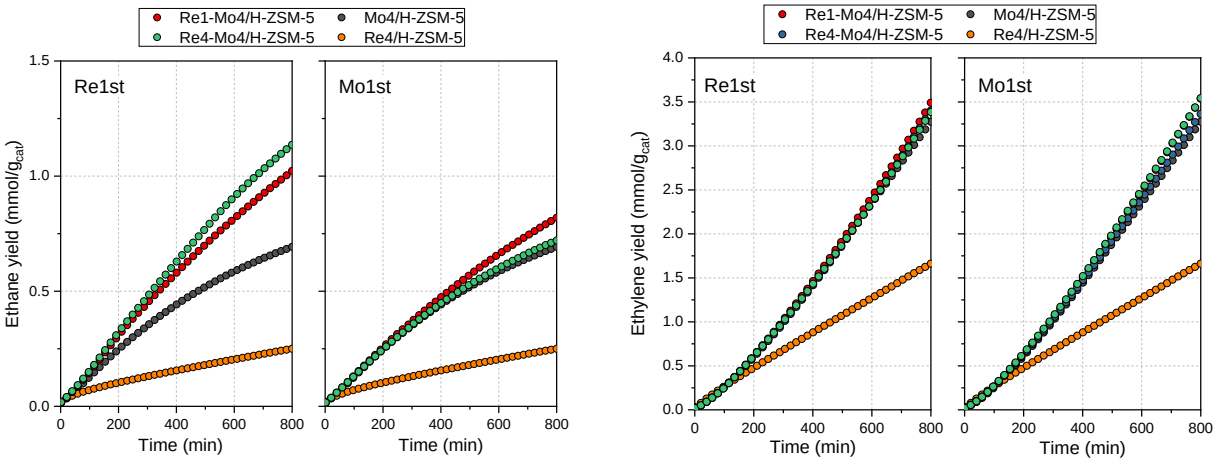

Figure 2. Evolution of accumulated ethane and ethylene formed during aromatization reaction over different catalysts from both series.

Characterization of calcined and reduced catalysts

In order to delve into the origin of the observed differences in the catalytic behaviour of the Re-Mo bimetallic catalysts, the systems were submitted to structural, textural and electronic characterization.

As showed from N_2 adsorption-desorption isotherms (**Figure S2)**, the introduction of metal in the zeolite certainly affects to surface features of the catalyst. Thus, a slight decrease in the BET surface is observed for Mo and Re monometallic catalysts and occurs in both the micropore and the external surface areas in a similar way (**Figure 3).** Such decrease is largest in the case of Re4 monometallic system, where BET surface area changes from 360 m^2/g for the ZSM-5 to 231 m^2/g

for Re4/ZSM-5. This diminution in the BET surface area value is significantly lower than that exhibited by Mo4 sample. From this result it can be inferred that Re would percolate better than Mo inside the porous structure during calcination causing the pore blockage, particularly micropore ones [7,22]. This effect has been previously reported for Re-MFI system [23]. In this study, Lacheen *et al* stated that through thermal treatment of Re_2O_7/H-MFI mixtures, the selective grafting of isolated and stable Re-oxo species via Re_2O_7 (g) reactions with OH groups to form $Si{-}O_fReO_3{-}Al$ (where O_f is framework O) is achieved. Moreover, grafting onto exchange sites would prevent the ubiquitous sublimation of ReO_x species.

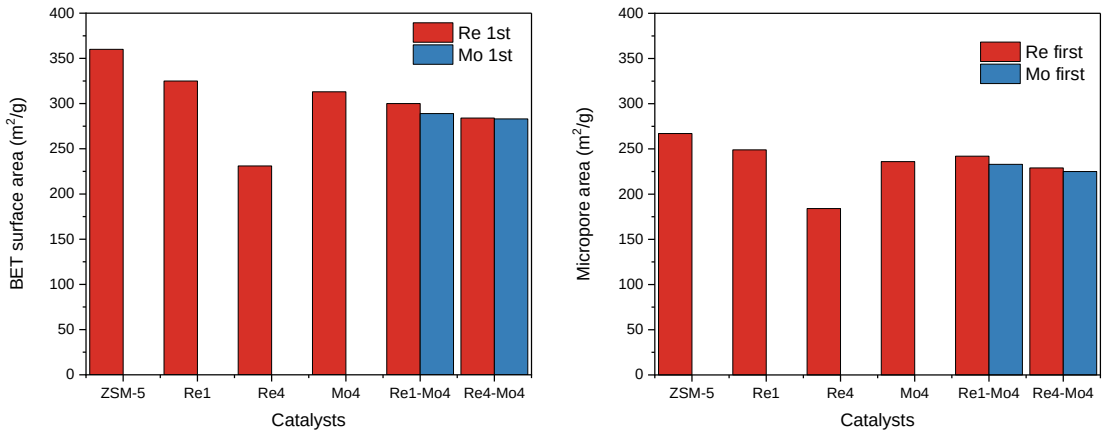

Figure 3. BET and micropore area results for the different catalysts prepared by both sequential methods.

It is surprising that bimetallic systems show similar surface features than monometallic Mo4/ZSM-5. Therefore, it appears that the changes in the surface area values are not related with the total metal loading. Moreover, the particular pore obstruction observed for monometallic Re seems not to be present in these bimetallic samples. The surface area of Re4/ZSM-5 is smaller than that of Re4-Mo4 catalyst, for which the metal loading is nearly double. Only a gradual decrease in the surface area with the total metal load increase is observed. In this sense, we have to consider that

in the case of Re4-Mo4/ZSM-5 (Re1st) the sample is submitted to a second calcination upon Mo impregnation that could help Re to diffuse. In the case of Re4-Mo4/ZSM-5 (Mo1st), the inner pores would be firstly occupied by Mo, leading Re in the outer sites. On this basis, in neither case, the micropore surface area wouldn't exhibit a comparable situation as Re4/ZSM-5.

Comparing the Re-Mo systems between the two series, it can be noticed that the introduction of Mo first (Mo1st series) led to a slightly lower surface area values than when Re is firstly impregnated (Re1st series). As a consequence of the observed evolution, we may infer that initial drastic pore obstruction by Re ions is not taking place in Re1st series. Indeed, for these samples, once Re is impregnated the solid is submitted to a further calcination process upon Mo incorporation. If we consider the high mobility of Re at moderate temperatures, it can be assumed that ions located at the inner micropore sites could be extracted and occupy the external surface or even partially sublimate. On the other side, when Re is incorporated in second place, it could be preferentially deposited close to Mo in close interaction as will be further discussed. This could explain that bimetallic samples do not show important diminution in the surface area. In spite of the different impregnation procedure, we have evidenced from HADDF a good dispersion of Re ions on the zeolite support (**Figure S3**). This fact denotes that Re would easily diffuse through zeolite pore structure upon different calcination treatments.

Adsorption microcalorimetry is a sensitive technique which provides a detailed description of both the quantitative and energetic features of the surface sites. Ammonia was used as the probe molecule for determining the total number, strength and strength distribution of surface acid sites. The differential heat of ammonia adsorption at 80 ºC on selected catalysts is presented in **Figure 4.a** as a function of surface coverage. The populations of the surface acid sites at various heat intervals of adsorption are shown in **Figure 4.b**. For all samples, after outgassing at 80 °C, NH_3

readsorption occurred only to a limited extent and with low values of differential heat of adsorption (Q_{diff} from 100 kJ/mol down to 60 kJ/mol). This indicates that the sites characterized by $Q_{diff} \leq$ 100 kJ/mol are weak enough to readily desorb ammonia molecules adsorbed during the first adsorption run. Therefore, they can be classified as weak. By observing the different distribution of sites for weak, medium and strong acid sites it can noted that the incorporation of metals largely affects the weak acid sites. Moreover, it can be pointed out that Mo incorporation only affects these weak sites (60-100 kJ/mol). When Re is present, it is worthy to note that stronger sites (> 100 kJ/mol) are specifically affected.

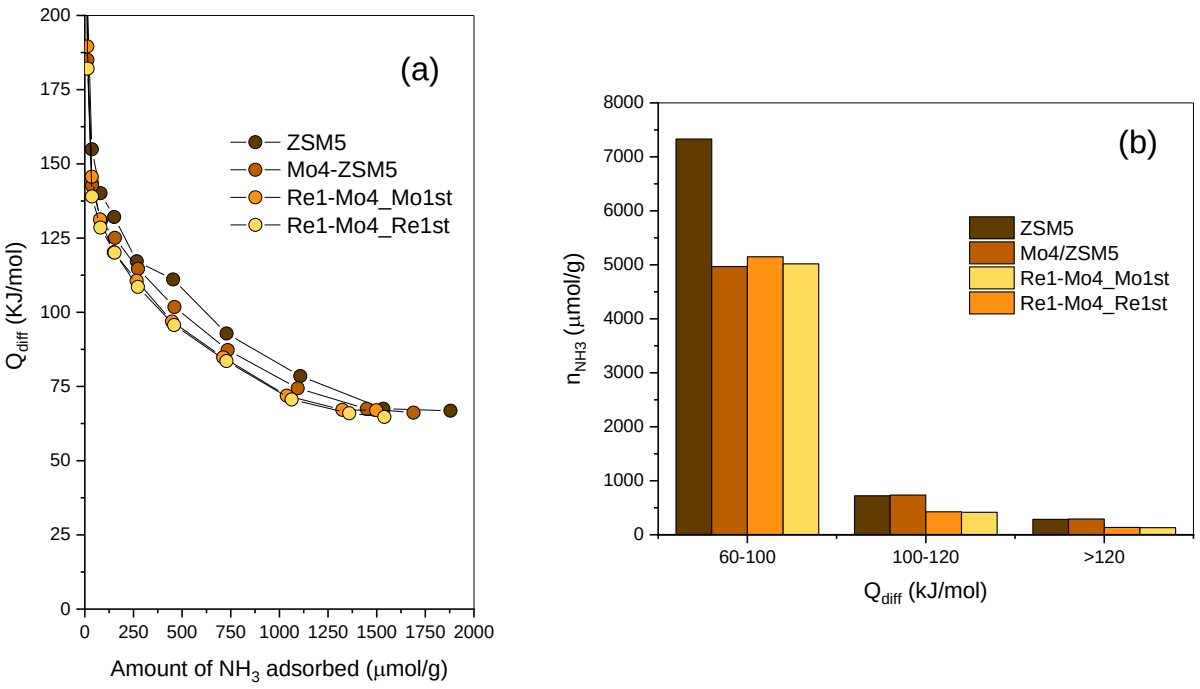

Figure 4. a) Differential heat of ammonia adsorption and b) Acid sites strength distribution obtained from ammonia adsorption for different catalysts.

In addition, it can be said that the sequence of metal incorporation in bimetallic systems would not have a clear effect on the number of these stronger acid sites. From these results, it can be argued

that Re naturally tends to occupy the strongest sites while Mo the weakest ones. Such differential behaviour could be related with the different acid character of the Mo and Re ions. In a recent work, Gao *et al* described that the strong interaction between acidic proton and Mo sites correlates with the products formation and catalyst lifetime [24]. These authors argued that this issue would have an important implication in modulating the catalytic MDA performance by taking advantage of the proximity of the acidic proton-Mo sites at atomic-level. Furthermore, Wang *et al* argued that tuning the surface acidity of charged catalyst would balance the aromatization performance and coke resistance for stability enhancement [25]. Thus, as they reported, the strong Lewis and Brønsted acidity of Ag/ZSM-5 would be closely related to its good catalytic performance towards aromatization.

Thus, in our case, as stated from microcalorimetry, such stronger acid sites would be occupied by Re ions that would condition Mo location and therefore favour the interaction with these acid sites. This fact would be associated to the particular ethane evolution observed (**Figure 2**).

Figure 5 depicts the TPR profiles obtained for the samples. As we have shown in previous works [26,27], Mo4/ZSM-5 sample showed a complex TPR profile. Such complexity that is denoted from TPR profile renders quite difficult the identification of the active site for this reaction [28]. In this sense, Kosinov et al. concluded that MoC_x species inside zeolite channels are the active sites, whereas MoC_x particles on the zeolite outer surface are "spectators" that only produce coke [4]. However, later they reassigned the active sites from MoC_x to single Mo atoms [29], which shows the intricacy of this question.

Thus, we proposed the occurrence of different molybdenum oxides species, that changed as the metal loading increases. Essentially, we reported four main reduction processes for this monometallic Mo sample (whose reducing processes peaked are at 510 ºC, 615 ºC, 755 ºC and

1000 ºC), showing the high heterogeneity of the chemical states of molybdenum supported on zeolite. On the other hand, Re reduction is much simpler and only one defined reduction peak is observed at ca. 400 ºC (**Figure S4**).

In the case of bimetallic catalysts, the reduction profile is quite different from monometallic references and cannot be represented as the sum of the two profiles. This fact would point out that certain Mo-Re interaction is present. Such assumption would also be in agreement with the particular evolution of surface feature discussed above (**Figure 3**). Moreover, particularly for Re1-Mo4 systems, it appears that metal introduction sequence also affects to the reduction profile. Thus, for this catalyst from Re1st series (**Figure 5**) the sharp peak associated to Re reduction appears shifted to a slightly higher temperature with lower intensity and showing a new notable shoulder. At the same time, most of the reduction peaks associated to Mo appeared in certain extent diminished. This change in the TPR profile would imply a different reorganization of Mo ions in the structure with respect to the monometallic system. As we have previously stated [26], the highest reduction temperature (ca. 1000 ºC) has been associated to small clusters of well-dispersed Mo monomers located at the inner microporous channels of the zeolite. As we have discussed, the role of these species would be similar to those small clusters of well-dispersed Mo monomers located on the external surface of the zeolite and would show certain activity. Therefore, the diminution of this particular reduction peak would be associated to the presence of Re ions that could avoid in part the insertion and formation of Mo small clusters at these inner sites. However, the observed diminution of these Mo-species seems not to affect notably the catalytic performance for bimetallic systems.

Moreover, the new important reduction process at ca. 450 ºC together with the partial disappearance of Mo reduction peaks would indicate that Mo is reduced at lower temperatures in

the presence of Re. It is worthy to mention that Re1-Mo4/ZSM-5 sample from Re1st series showed a more marked different profile with respect to monometallic Mo4/ZSM-5. Thus, in addition to the identified Mo active sites, new active sites probably associated to Re-Mo entities are expected and would be responsible of the improved performance.

We could infer that main diminution in the TPR profile is attained in the region 800 - 920 ºC (**Figure 5**). If we consider the different species described in a previous work, this reduction temperature range would be associated to external located bulk-like MoO_3. From HAADF images we unequivocally showed that these species would be supported on aluminium oxide segregated from the zeolite network and would be responsible of the heavy coke formation [26]. The particular modifications observed in this sample were not so marked for the same catalyst in the Mo1st series (**Figure 5**); so, the different sequential deposition clearly induces a different structural situation. For this series, it seems that the TPR peak that appeared more affected was that at higher temperature. Thus, reduction peak has been associated to the well dispersed Mo-monomers located at the inner micropores with strong interaction with the support. The diminution of this reduction peak in this series would point out that upon Re incorporation these Mo species would diffuse to other positions, becoming easily reducible.

In the case of Re4-Mo4 catalysts, the TPR profiles do not show important differences between the two series. It is worthy to note that, in spite of the higher Re loading with respect to Re1-Mo4 catalysts, the low temperature peak in principle associated to Re reduction appears with similar intensity as in the case of Re1-Mo4 catalysts. This fact would denote that the reduction would not be complete.

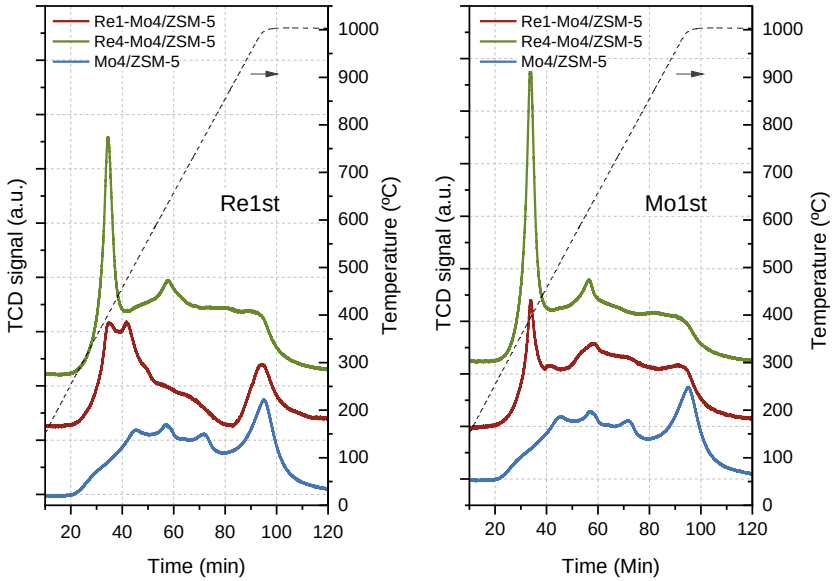

Figure 5. TPR profiles of monometallic Mo4/ZSM-5, and bimetallic Re-Mo/ZSM-5 catalysts from both series.

If we consider the metal content for both series (**Table 1**), it is worthy to note that while Mo content appears in all cases close to the nominal one, in the case of Re it can be noticed that for Re1st series the metal content is lower. This fact could be related with the high mobility of Re previously mentioned. Indeed, it has been reported that Re_2O_7 sublimation would occur at 250 ºC [30]. This fact has been used for achieving stable Re-oxo species grafted on zeolite precursors via Re_2O_7 (g) reactions with OH groups [23]. That issue has been pointed out from surface acidity discussion.

Indeed, for Re1st series the second calcination after Mo impregnation would provoke certain metal sublimation that lead to the slight metal loading diminution. Moreover, this process would explain why inner micropores that initially were blocked became free after the second calcination

due to the migration toward the external surface. Such high mobility of Re ions would play an important role in the explanation of TPR profiles above discussed.

From H_2 consumption and considering the metal content observed from ICP-OES analysis, we have also calculated the variation in the oxidation state for the supported metals (**Table 1**). In the case of monometallic samples, the obtained reduction degrees highlight that after TPR treatment, metal ions were fully reduced from +6 and +7 oxidation state for Mo and Re monometallic catalysts respectively.

Table 1. Metal content and H_2 consumption from TPR and oxidation state variation for Re-Mo/ZSM-5 from both series.

	Catalysts	Re wt% *	Mo wt% *	μmol H_2/mg_{cat}	Average reduction %
	Mo4/ZSM-5	---	4.2	1.16	88
	Re1/ZSM-5	1.3	---	0.23	93
	Re4/ZSM-5	3.6	---	0.66	97
Re1st	Re1-Mo4/ZSM-5	0.8	4.2	0.98	67
	Re4-Mo4/ZSM-5	2.3	3.8	1.43	91
Mo1st	Re1-Mo4/ZSM-5	1.2	3.8	1.25	99
	Re4-Mo4/ZSM-5	3.0	3.8	1.36	81

* *Metal content from ICP-OES analysis*.

On the other hand, by observing the reduction degree for the bimetallic systems it is clear that Re1-Mo4/ZSM-5 from Re1st series would show a particular behaviour. For this catalyst, a fraction of the metal content would remain partially oxidized (67% of ions are reduced). This would clearly imply the coexistence of Re-Mo species that are stabilized in a partially oxidized state. Such behaviour is not observed in the similar catalyst from Mo1st series or even for Re4-Mo4 catalysts. Therefore, the order in the sequential incorporation notably affects the final structural and chemical feature of metals.

In **Figure 6** we show the XPS Mo *3d* and Re *4f* spectra for all samples after soft oxidation at 250 ºC. The binding energy for Mo $3d_{5/2}$ in Mo4/ZSM-5 is located at 233.3 eV, which has been reported for Mo^{6+} in MoO_3 [31,32]. On the other hand, in the case of Re4/ZSM-5 the observed binding energy for Re $4f_{7/2}$ level is 46.1 eV, which is in accordance with values associated to Re^{7+} [33].

In the case of bimetallic Re1-Mo4/ZSM-5 catalysts, Mo *3d* and Re *4f* bands show a slight shift toward lower binding energy values. Such small shift would point out a strong interaction with Re. Indeed, as above discussed, from TPR experiments we have denoted a different reduction profile and a lower reduction degree in the case of Re1st series. Additionally, from BET surface area and acidity measurements we also pointed out such possibility. Thus, when rhenium is present it can be assumed that Mo and Re form a new entity in close interaction.

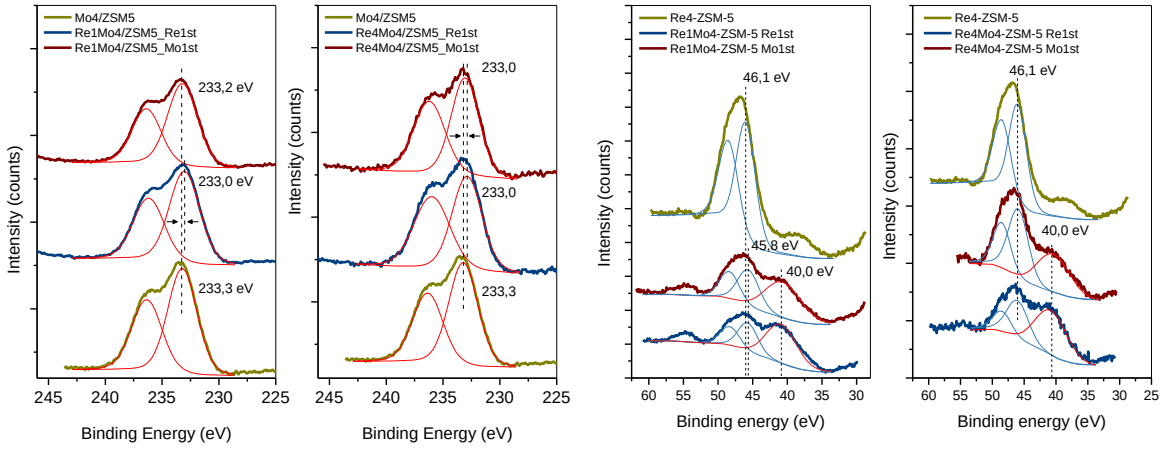

Figure 6. XPS Mo *3d* and Re *4f* core-level spectra for monometallic and bimetallic Mo-Re/ZSM-5 catalysts after soft oxidation at 250 ºC.

If we consider the surface composition (**Table S1**), it can be noticed that in the case of Mo similar Mo/Si ratios were obtained for all catalysts, being in all cases close to Mo content in the monometallic one. However, for rhenium the surface content for Re4-Mo4 in the Re1st series lies markedly below the reference value of monometallic one (0.013 vs 0.007 for Re4/ZSM-5 and R4-Mo4/ZSM-5 Re1st, respectively). The observed differences could be related in principle to a different surface content probably due to a certain loss of Re during the second calcination but, more importantly, to a different distribution of rhenium ions due to the second calcination treatment. In order to confirm the above behaviour we have studied the evolution of the surface during reduction treatment. The results obtained by an *in situ* XPS study of the reduction process of the monometallic (Mo4/ZSM-5 and Re4/ZSM-5) and bimetallic catalysts from both series are shown below.

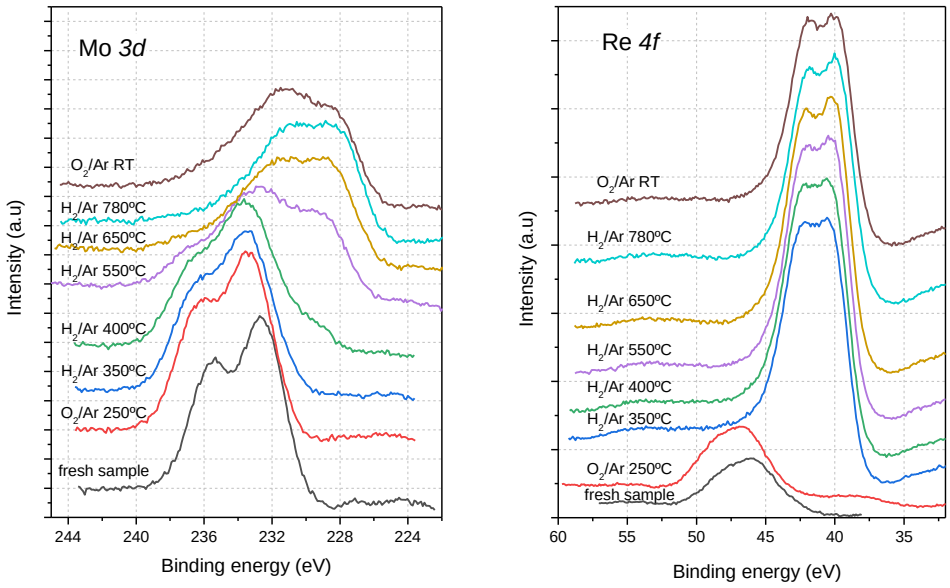

Figure 7. Mo *3d* and Re *4f* regions XPS spectra for the Mo4/ZSM-5 and Re4/ZSM-5 monometallic catalyst calcined and after *in situ* reduction treatment.

The Mo *3d* and Re *4f* regions spectra obtained along different reduction treatments of the monometallic Mo4/ZSM-5 and Re4/ZSM-5 systems are shown in **Figure 7**. As previously indicated, for Mo system the only oxidation state present after evacuation pretreatment in O_2 is Mo^{6+} (**Figure 7**). Upon reduction, the Mo *3d* peak doublet becomes less defined, pointing out the co-existence of other species as it was stated from the complex TPR profile. Just after reduction at 650 ºC, the Mo *3d* peak becomes wider and clearly shifted to lower BE (being Mo $3d_{5/2}$ at ca. 228.0 eV), denoting that surface Mo is almost reduced to Mo^0 (**Table S1**). Therefore, it can be said that at this temperature all Mo species at the surface got reduced. On the other hand, regarding to Re4/ZSM-5, after calcination the wide peak located at ca. 46.1 eV would denote that the main oxidation state is +7 (**Figure 6**). As observed from TPR, total reduction is achieved at a

significantly lower temperature. Indeed, after reduction treatment at 350 ºC the Re $4f_{7/2}$ peak at 40 eV clearly points out the complete reduction of Re. It is also worthy to note that the intensity of this peak is notably higher than that for calcined sample. Thus, it is evidenced that upon reduction a notable Re surface enrichment is taking place (**Figure 7**).

The evolution of Re-Mo bimetallic catalysts upon reduction is shown in **Figures 8** and **9**. In the case of molybdenum, Re1-Mo4 and Re4-Mo4 catalysts follow similar reduction evolution within each different series (**Figure 8** and **9**). Mo reduction is taking place in both series at slightly lower temperature with respect to that observed for Mo-monometallic catalyst. Irrespective of the Re amount or addition sequence, contributions of reduced Mo species can be seen at 400 ºC. On the other hand, in the case of Re almost complete reduction is achieved upon treatment at 350 ºC, which agrees with the behaviour observed for monometallic Re catalyst.

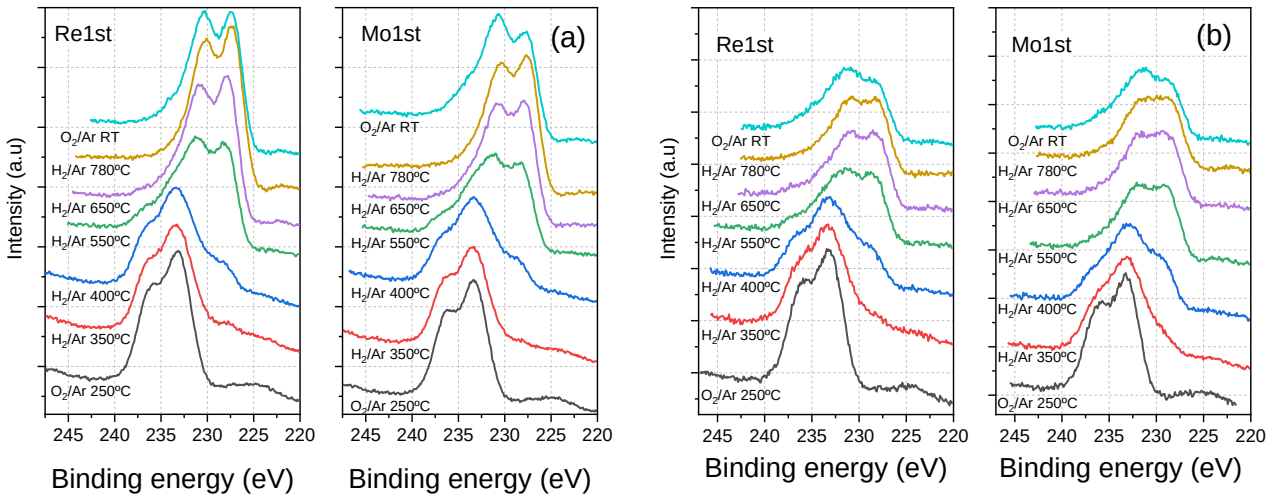

Figure 8. Mo *3d* region XPS spectra for a) Re1-Mo4/ZSM-5 catalysts and b) Re4-Mo4/ZSM-5 catalysts from both series calcined and after in *situ* reduction.

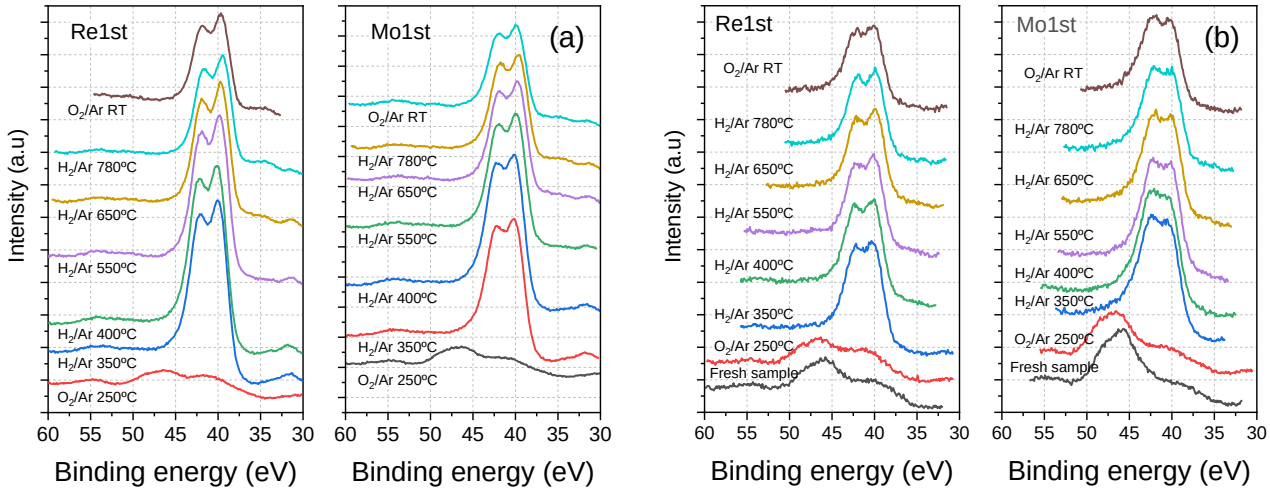

Figure 9. Re *4f* region XPS spectra for a) Re1-Mo4/ZSM-5 catalyst and b) the Re4-Mo4/ZSM-5 catalyst from both series calcined and after in *situ* reduction. (Notice that Mo *2p* peak appears at the same region than Re *4f)*.

As previously pointed out for monometallic systems, an important Re enrichment can be also observed in these bimetallic systems. In **Figure 10** we have plotted the evolution of Re/Si and Mo/Si ratios for all catalysts along with the reduction treatment. As a general trend, we can state that surface Re/Si ratio seems to increase in the first stage of reduction treatment, after which it starts to decay. This would point out that after the first surface enrichment, a slight loss of Re by sublimation, or even certain aggregation forming higher size clusters, occurs.

On the contrary, for Mo/Si ratio more stable evolution is attained though certain slight decrease can be observable for monometallic catalyst and more markedly for Re4-Mo4 bimetallic catalysts.

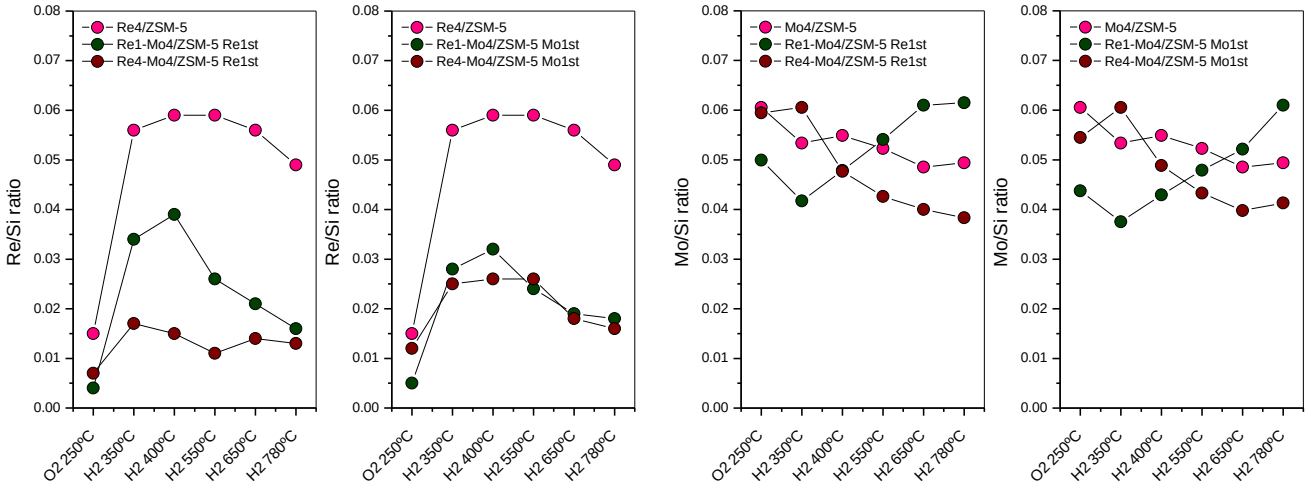

Figure 10. Evolution of the Re/Si and Mo/Si surface ratios upon reduction treatment.

It is worthy to note that for Re1-Mo4 the evolution is the opposite, as Mo/Si surface ratio exhibits a progressive increase. This would indicate that Mo clusters could be dispersed upon reduction in the presence of Re. From these results it is clear that the surface follows a complex evolution during reduction at different temperatures and that the presence of Re would strongly affect the behaviour of Mo upon reaction conditions, denoting the observed strong interaction of both metals. Thus, Mo would show certain dispersion/enrichment for Re1-Mo4/ZSM-5 while it would suffer aggregation as reduction temperature increases for Re4-Mo4. This later aggregation would be associated to the formation of Mo-Re species, as was discussed from TPR results.

All this particular structural surface and chemical features showed by bimetallic Re-Mo with respect to monometallic Mo system that has been widely discussed along this study could be correlated with the different catalytic behaviour observed for bimetallic catalysts, particularly with low Re content. Within this context, the sequential impregnation would also play an important

role, unblocking inner micropores during second calcination and favouring a close Re-Mo interaction that would lead to Re-Mo stabilized against reduction.

CONCLUSIONS.

The incorporation of rhenium as co-dopant to the Mo/ZSM-5 catalyst has shown a notable improvement in the *MDA* reaction. Benzene/aromatics yields for bimetallic systems appear significantly enhanced. Moreover, the catalytic performance of bimetallic systems is clearly affected by the sequence addition of metals. Thus, the best catalytic behaviour has been attained for Re1-Mo4/ZSM-5 in which Re has been firstly deposited (Re1st series).

Due to the high mobility of Re ions, for the Re1st series Re would undergo a particular evolution that affects the further Mo incorporation. This fact has been stated through the wide surface and structural characterization of the systems. Based on these results, we evidenced that Re ions would be preferentially located at strong acid sites. This fact modifies also the state of Mo species, which showed a close interaction with Re entities. As a result, the C-C coupling step would be favoured, which seems to be the responsible for the catalytic performance improvement. Indeed, as we have evidenced, the formation of ethylene is similar for all systems and therefore seems not to be related with the presence of Re. Thus, the higher aromatics yield would be directly related to the higher ethane formation.

ASSOCIATED CONTENT

Supporting Information. It is available in a separate file.

AUTHOR INFORMATION

Corresponding Author

Email: gcolon@icmse.csic.es

Present Addresses

Instituto de Ciencia de Materiales de Sevilla (CSIC-University of Seville) and Departamento de Química Inorgánica. University of Seville. Av. Américo Vespucio. 49. 41092 Seville. Spain

ACKNOWLEDGMENT

We thank the "Ministerio de Economía and Competitividad" of Spain (Projects ENE2017-88818-C2-1-R and CTQ2014-60524-R). The EU FEDER program and the "Junta de Andalucía" (Project US-1263455 and FQM015 group) for financial support.

REFERENCES

[1] L. Wang, L. Tao, M. Xie, G. Xu, J. Huang, Y. Xu, Dehydrogenation and Aromatization of Methane under Non-Oxidizing Conditions. Catal. Letters, 21 (1993) pp 35–41.

[2] J.N. Armor, Emerging Importance of Shale Gas to Both the Energy & Chemicals Landscape. J. Energy Chem., 22 (2013) pp 21–26.

[3] D. Kiani, S. Sourav, Y. Tang, J. Baltrusaitis, I.E. Wachs, Methane activation by ZSM-5-supported transition metal centers. Chem. Soc. Rev. 50 (2021) pp 1251–1268.

[4] N. Kosinov, E.A. Uslamin, F.J.A. Coumans, A.S.G. Wijpkema, R.Y. Rohling, E.J.M. Hensen, Structure and evolution of confined carbon species during methane dehydroaromatization over Mo/ZSM-5. ACS Catal. 8 (2018) pp 8459–84677.

[5] S.J. Han, S.K. Kim, A. Hwang, S. Kim, D.Y. Hong, G. Kwak, K.W. Jun, Y.T. Kim, Non-Oxidative dehydroaromatization of methane over Mo/H-ZSM-5 catalysts: A detailed analysis of the reaction-regeneration cycle. Appl. Catal. B Environ. 241 (2019) pp 305–318.

[6] C.H.L. Tempelman, E.J.M. Hensen, On the Deactivation of Mo/HZSM-5 in the Methane Dehydroaromatization Reaction. Appl. Catal. B Environ. 176–177 (2015) pp 731–739.

[7] Y. Gu, P. Chen, H. Yan, X. Wang, Y. Lyu, Y. Tian, W. Liu, Z. Yan, X. Liu, Coking mechanism of Mo/ZSM-5 catalyst in methane dehydroaromatization. Appl. Catal. A: Gen. 6135 (2021) 118019.

[8] U. Menon, M. Rahman, S.J. Khatib, A critical literature review of the advances in methane dehydroaromatization over multifunctional metal-promoted zeolite catalysts. Appl. Catal. A: Gen. 608 (2020) 117870.

[9] T.E. Tshabalala, N.J. Coville, M.S. Scurrell, Dehydroaromatization of methane over doped Pt/Mo/H-ZSM-5 zeolite catalysts : The Promotional Effect of Tin. Appl. Catal. A Gen. 485 (2014) pp 238–244.

[10] V. Abdelsayed, D. Shekhawat, M.W. Smith, Effect of Fe and Zn Promoters on Mo/HZSM-5 Catalyst for Methane Dehydroaromatization. Fuel 139 (2015) pp 401–410.

[11] Y. Zhang, M. Kidder, R.E. Ruther, J. Nanda, G.S. Foo, Z. Wu, C.K. Narula, Promotional effects of In on non-oxidative methane transformation over Mo-ZSM-5. Catal. Letters 146 (2016) pp 1903–1909.

[12] A. Sridhar, M. Rahman, A. Infantes-Molina, B.J. Wylie, C.G. Borcik, S.J. Khatib, Bimetallic Mo-Co/ZSM-5 and Mo-Ni/ZSM-5 Catalysts for Methane Dehydroaromatization: A Study of the Effect of Pretreatment and Metal Loadings on the Catalytic Behaviour. Appl. Catal. A Gen. 589 (2020) 117247.

[13] P. Schwach, X. Pan, X. Bao, Direct Conversion of Methane to Value-Added Chemicals over Heterogeneous Catalysts: Challenges and Prospects. Chem. Rev. 117 (2017) pp 8497–8520.

[14] A.M. Hilmen, D. Schanke, A. Holmen, TPR study of the mechanism of Rhenium promotion of alumina-supported Cobalt Fischer-Tropsch catalysts, Catal. Letters 38 (1996) pp 143–147.

[15] I. Vollmer, E. Abou-Hamad, J. Gascón, F. Kapteijn, Aromatization of Ethylene – Main Intermediate for MDA? ChemCatChem, 12 (2020) pp 544–549.

[16] A. Sridhar, M. Rahman, S. J. Khatib, Enhancement of Molybdenum/ZSM-5 Catalysts in Methane Aromatization by the Addition of Iron Promoters and by Reduction/Carburization Pretreatment. ChemCatChem 10 (2018) pp 2571 –2583.

[17] A. Sridhar, M. Rahman, A. Infantes-Molina, B.J. Wylie, C.G. Borcik, S.J.Khatib, Bimetallic Mo-Co/ZSM-5 and Mo-Ni/ZSM-5 catalysts for methane dehydroaromatization: A study of the effect of pretreatment and metal loadings on the catalytic behavior, App. Catal. A: Gen. 589 (2020) 117247.

[18] A. Sridhar, M. Rahman, A. Infantes-Molina, Be.J. Wylie, C.G. Borcik, S.J. Khati, Bimetallic Mo-Co/ZSM-5 and Mo-Ni/ZSM-5 catalysts for methane dehydroaromatization: A study of the effect of pretreatment and metal loadings on the catalytic behavior, Appl. Catal. A: Gen. 589 (2020) 117247.

[19] A. Galadima, O. Muraza, Advances in Catalyst design for the conversion of methane to aromatics: A critical review. Catal. Surv. Asia 23 (2019) pp 149–170.

[20] Y. Gu, P. Chen, H. Yan, X. Wang, Y. Lyu, Y. Tian, W. Liu, Z. Yan, X. Liu, Coking mechanism of Mo/ZSM-5 catalyst in methane dehydroaromatization, Appl. Catal. A: Gen. 613 (2021) 118019.

[21] N. K. Razdan, A. Kumar, B. L. Foley, A. Bhan, Influence of ethylene and acetylene on the rate and reversibility of methane dehydroaromatization on Mo/H-ZSM-5 catalysts. J. Catal. 381 (2020) pp 261–270.

[22] N. Kosinov, F.J.A.G. Coumans, G. Li, E. Uslamin, B. Mezari, A.S.G. Wijpkema, E.A. Pidko, E.J.M. Hensen, Stable Mo/HZSM-5 methane dehydroaromatization catalysts optimized for stable

Mo/HZSM-5 methane dehydroaromatization catalysts optimized for high-temperature calcination-regeneration. J. Catal. 346 (2017) pp 125–133.
[23] H.S. Lacheen, P.J. Cordeiro, E. Iglesia, Structure and catalytic function of Re-oxo species grafted onto H-MFI zeolite by sublimation of Re_2O_7. J. Am. Chem. Soc. 128 (2006) pp 15082-15083
[24] W. Gao, G. Qi, Q. Wang, W. Wang, S. Li, I. Hung, Z. Gan, J. Xu, F. Deng, Dual active sites on Molybdenum/ZSM-5 catalyst for methane dehydroaromatization: Insights from solid-state NMR spectroscopy. Angew. Chem. Int. Ed. 60 (2021) pp 10709–10715.
[25] A. Wang, P. He, M. Yung, H. Zeng, H. Qian, H. Song, Catalytic Co-Aromatization of Ethanol and Methane. Appl. Catal. B Environ. 2016, 198, 480–492.
[26] A. López-Martín, A. Caballero, G. Colón, Structural and surface considerations on Mo/ZSM-5 systems for methane dehydroaromatization reaction. Mol. Catal. 486 (2020) p 110787.
[27] A. López-Martín, F. Platero, G. Colón, A. Caballero, Elucidating the nature of Mo species on ZSM-5 and its role in the methane aromatization reaction. React. Chem. Eng. 6 (2021) pp 1265–1276.
[28] N. Wang, X. Dong, L. Liu, D. Cai, Q. Cheng, J. Wang, Y. Hou, A.H. Emwas, J. Gascon, Y. Han, Probing the Catalytic Active Sites of Mo/HZSM-5 and Their Deactivation during Methane Dehydroaromatization, Cell Rep. Phys. Sci. 2 (2021) 100309.
[29]N. Kosinov, A.S.G. Wijpkema, E. Uslamin, R. Rohling, F.J.A.G. Coumans, B. Mezari, A. Pa rastaev, A.S. Poryvaev, M.V. Fedin, E.A. Pidko, E.J.M. Hensen Confined carbon mediating dehydroaromatization of methane over Mo/ZSM-5 Angew. Chem. Int. Ed. Engl., 57 (2018) pp. 1016-1020.
[30] T. Otsuka, N. Sawano, Y. Fujii, T. Omura, C. Taylor, M. Shimada, Effects of rhenium contents on oxidation behaviours of tungsten-rhenium alloys in the oxygen gas atmosphere at 873 K. Nucl. Mater. Energy 25 (2020) 1007913.
[31] J.-G. Choi, L.T. Thompson, XPS study of as-prepared and reduced molybdenum oxides. Appl. Surf. Sci. 93 (1996) pp 143–149.
[32] T. Schroeder, J. Zegenhagen, N. Magg, B. Immaraporn. H.-J. Freund, Formation of a faceted MoO_2 epilayer on Mo(1 1 2) studied by XPS, UPS and STM. Surf. Sci. 552 (2004) pp 85–97.

[33] V.V. Kuznetsov, Y.D. Gamburg, V.V. Zhulikov, R.S. Batalov, E.A. Filatova, Re-Ni cathodes obtained by electrodeposition as a promising electrode material for hydrogen evolution reaction in alkaline solutions. Electrochim. Acta 317 (2019) pp 358–366.